

Metallicity Estimates for Old Star Clusters in M33

Jun Ma, Xu Zhou and Jiansheng Chen

National Astronomical Observatories, Chinese Academy of Sciences, Beijing, 100012, P.R. China

Received 18 February 2003 / Accepted 7 August 2003

Abstract. Using the theoretical stellar population synthesis models of BC96, Kong et al. (2003) showed that some BATC colors and color indices could be used to disentangle the age and metallicity effect. They found that there is a very good relation between the flux ratio of L_{8510}/L_{9170} and the metallicity for stellar populations older than 1 Gyr. In this paper, based on the Kong et al. results and on the multicolor spectrophotometry of Ma et al. (2001, 2002a,b,c), we estimate the metallicities of 31 old star clusters in the nearby spiral galaxy M33, 23 of which are “true” globular clusters. The results show that most of these old clusters are metal poor. We also find that the ages and metal abundance for these old star clusters of M33 do not vary with deprojected radial position.

Key words. galaxies: individual M33 – galaxies: evolution – galaxies: star clusters

1. Introduction

Globular clusters (GCs) are thought to be among the oldest radiant objects in the Universe. They are simple coeval stellar systems which formed on a very short timescale during phases of intense star formation in host galaxies. The GCs of the Milky Way probe the manner in which our Galaxy formed. Studies of similar populations in other galaxies can reveal the properties of these galaxies soon after their formation. For example, the widely varying specific frequency of GCs in individual galaxies indicates that cluster formation is almost certainly affected by the local environment with the host galaxy.

M33, at a distance of 850 kpc, is the third-brightest member of the Local Group, and is classified as a late-type ScII-III spiral (van den Bergh 1999). This galaxy represents a morphological type intermediate between the largest “early-type” spirals and the dwarf irregulars in the Local Group (Chandar, Bianchi, & Ford 1999a). M33 subtends 1° on the sky. Its large angular extent and favorable inclination $i = 56^\circ$ (Regan & Vogel 1994) make it suitable for studies of stellar content. However, its large size makes its study difficult. The Beijing-Arizona-Taiwan-Connecticut (BATC) Multicolor Sky Survey (Fan et al. 1997; Zheng et al. 1999) observes M33 as part of its galaxy calibration program.

Before Chandar et al. (1999a, 1999b, 1999c, 2001, 2002), the system of clusters in M33 were not be well studied, although detection, and photometry and spectrophotometry have been obtained (see details from Hiltner 1960; Kron & Mayall 1960; Melnick & D’Odorico 1978; Christian

& Schommer 1982, 1988; Huchra et al. 1996). Now, a database of about 400 star clusters is available from the ground-based work, and from the *Hubble Space Telescope* (HST) images.

Using the theoretical stellar population synthesis models of Bruzual & Charlot (1996, unpublished, hereafter BC96) and multicolor photometry, Kong et al. (2000) studied the age, metallicity, and interstellar-medium reddening distribution for M81. When they convolved the spectral energy distributions (SEDs) of BC96 with the BATC filter profiles to obtain the optical and near-integrated luminosity, they found that, among all the BATC filter bands, the color index centered at 8510Å is much more sensitive to the metallicity than to the age. The center of this filter band is near the Ca II triplets ($\lambda\lambda = 8498, 8542, 8662\text{Å}$) (hereafter CaT). As Zhou (1991) noted, that the strength of the CaT depends on the effective temperature, surface gravity, and the metallicity in late-type stars. A very good relation between the flux ratio of $I_{8510} \equiv L_{8510}/L_{9170}$ and the metallicity was found for stellar populations older than 1 Gyr in Kong et al. (2000).

In this paper, we estimate the metallicities of the 31 old star clusters that were detected by Christian & Schommer (1982), Chandar, Bianchi, & Ford (1999a, 2001), and by Mochejska et al. (1998) in M33 using the relation of Kong et al. (2000). The ages of all these sample star clusters were estimated by Ma et al. (2001, 2002a, 2002b, 2002c) by comparing the BC96 simple stellar population synthesis models with the integrated photometric measurements.

The outline of the paper is as follows. Sample selection, observations and data reduction are given in section 2. Section 3 presents the spectral synthesis models. In section

Send offprint requests to: Jun Ma,
e-mail: majun@vega.bac.pku.edu.cn

4, we provide a brief description of the method of Kong et al. (2000), and estimate the metallicities of 31 sample old star clusters. Some statistical properties of old star clusters are investigated in section 5. In section 6, we give our major results and some discussions.

2. Sample of star clusters, observations and data reduction

2.1. Sample of old star clusters

The sample of star clusters in this paper is from Ma et al. (2001, 2002a,b,c), who presented multicolor photometry and estimated the ages using BC96 models for 180 star clusters in M33. The RA and Dec of these clusters are from Christian & Schommer (1982), Chandar, Bianchi, & Ford (1999a, 2001), or Mochejska et al. (1998). Christian & Schommer (1982) detected more than 250 nonstellar objects using 14×14 inch² unfiltered, unbaked, IIa-O focus plates exposed for 150 minutes with the Kitt Peak 4 m Richey-Chrétien (R-C) direct camera. Chandar, Bianchi & Ford (1999a, 2001) used 55 multiband HST WFPC2 fields to search for star clusters much closer to the nucleus of M33 than previous studies, and detected 162 star clusters, 131 of which were previously unknown. Mochejska et al. (1998) detected 51 globular cluster candidates in M33, 32 of which were not previously cataloged, using the data collected in the DIRECT project (Kaluzny et al. 1998; Stanek et al. 1998). Ma et al. (2001, 2002a,b,c) obtained the SEDs of the 180 clusters by aperture photometry, and estimated their ages using the theoretical evolutionary population synthesis methods. In Ma et al. (2001), there are 10 clusters, the ages of which are older than 1 Gyr. We exclude three star clusters of these 10 because of their low signal-to-noise ratios. Also, cluster 54 in Chandar, Bianchi, & Ford (1999a) is U137 in Christian & Schommer (1982). In Ma et al. (2002b), there are 22 clusters older than 1 Gyr. However, the ratios of signal-to-noise of 11 clusters are not high enough, and are not included in this sample. In Ma et al. (2002c), there are 5 clusters older than 1 Gyr. The signal-to-noise ratio of cluster 2 is not high enough, and is also not included in this sample. Altogether, there are 31 old star clusters in this paper. Figure 1 is the image of M33 in filter BATC07 (5785Å), the circles indicate the positions of the sample clusters. By comparing the photometric measurements to integrated colors from theoretical models by Bertelli et al. (1994), Chandar et al. (1999b, 2002) estimated ages for 23 old star clusters in common. Table 1 lists the comparison of age estimates with previously results (Chandar et al. 1999b, 2002). Except for clusters 49 and 59 of Chandar et al. (1999a), the ages estimated by Ma et al. (2001, 2002a,b,c) are consistent with the ones estimated by Chandar et al. (1999b, 2002). Cluster 49, the $B - V$ value of which is very large 0.824 (Chandar et al. 1999b), should be an old cluster. Our sample includes 23 “true” globular clusters, which have $(B - V)_0 \geq 0.6$ or

Fig. 1. The image of M33 in filter BATC07 (5785Å) and the positions of the sample star clusters. The center of the image is located at RA = 01^h33^m50^s.58 Dec=30°39'08".4 (J2000.0). North is up and east is to the left.

$(V - I)_0 \geq 0.78$, colors typical of Galactic GCs (Chandar, Bianchi, & Ford 2001).

2.2. Observations and data reduction

The large field multicolor observations of the spiral galaxy M33 were collected using the Ford Aerospace 2048 × 2048 CCD mosaic camera on the 60/90 cm f/3 Schmidt telescope of the Xinglong station of the National Astronomical Observatories. The field of view of the CCD is 58' × 58' with a pixel scale of 1''.7. The typical seeing of the Xinglong station is 2''. The multicolor BATC filter system, which was specifically designed to avoid contamination from the brightest and most variable night sky emission lines, includes 15 intermediate-band filters, covering the total optical wavelength range from 3000 to 10000Å. It is defined the magnitude zero points similar to the spectrophotometric AB magnitude system, a \tilde{F}_ν monochromatic system (Oke & Gunn 1983) based on the SEDs of the four F sub-dwarfs, HD 19445, HD 84937, BD +26°2606, and BD +17°4708. The advantage of the AB magnitude system is that the magnitude is directly related to physical units. The BATC magnitude system is defined as the AB magnitude system,

$$m_{\text{batc}} = -2.5 \log \tilde{F}_\nu - 48.60, \quad (1)$$

where \tilde{F}_ν is the appropriately averaged monochromatic flux in units of $\text{erg s}^{-1} \text{cm}^{-2} \text{Hz}^{-1}$ at the effective wavelength of the specific passband. In the BATC system (Yan et al. 1999), \tilde{F}_ν is defined as

$$\tilde{F}_\nu = \frac{\int d(\log \nu) f_\nu R_\nu}{\int d(\log \nu) R_\nu}, \quad (2)$$

which links the magnitude to the number of photons detected by the CCD rather than to the input flux (Fukugita

et al. 1996). In this equation, R_ν is the system response, f_ν is the SED of the source.

The images of M33 covering the whole optical body of M33 were accumulated in 13 intermediate band filters with a total exposure time of about 37.25 hours from September 23, 1995 to August 28, 2000. Data reduction, by bias subtraction and flat-fielding with dome flats, was performed with the automatic data reduction software PIPELINE I developed for the BATC multicolor sky survey (Fan et al. 1996; Zheng et al. 1999). The dome flat-field images were taken by using a diffuse plate in front of the correcting plate of the Schmidt telescope. We performed photometric calibration of the M33 images using the Oke-Gunn primary flux standard stars HD 19445, HD 84937, BD +26°2606, and BD +17°4708, which were observed during photometric nights (see details from Yan et al. 1999; Zhou et al. 2001).

Using the images of the standard stars observed on photometric nights, we derive iteratively the extinction curves and the slight variation of the extinction coefficients with time (Zhou et al. 2001). The extinction coefficients at any given time in a night [$K + \Delta K(UT)$] and the zero point of the instrumental magnitude (C) were obtained by

$$m_{\text{batc}} = m_{\text{inst}} + [K + \Delta K(UT)]X + C, \quad (3)$$

where X is air mass. The instrumental magnitudes (m_{inst}) of the selected bright, isolated and unsaturated stars on the M33 images of the same photometric nights can be readily transformed to the BATC AB magnitude system (m_{batc}). We calibrated the photometry on the combined images by comparing the magnitudes of these stars to determine a mean magnitude offset to the photometric images. Table 2 lists the parameters of the BATC filters and the statistics of observations. Column 6 of Table 2 gives the zero point error, in magnitude, for the standard stars in each filter. The formal errors we obtain for these stars in the 13 BATC filters are $\lesssim 0.02$ mag. This indicates that we can define the standard BATC system to an accuracy of $\lesssim 0.02$ mag.

2.3. Integrated photometry

For each star cluster, aperture photometry was used to obtain magnitudes. To avoid contamination from nearby objects, we adopt a small aperture of 6.8" corresponding to a diameter of 4 pixels in the Ford CCD. The large-aperture measures on the uncrowded bright stars were used to determine the aperture corrections, i.e., the magnitude difference between the small-aperture magnitude and the “total” or seeing-independent magnitude for the stars on each frame. The uncertainties for each filter take into account the error from the object count rate, sky variance, and instrument gain. For convenience, we present Table 3 with multiband photometry for sample clusters in this paper based on Ma et al. (2001, 2002a,b,c). Column 1 is cluster number. Column 2 to Column 14 show the magnitudes of different bands. The second line of each star

cluster is the uncertainties of magnitude of corresponding band.

3. Spectral synthesis

Since the pioneering works of Tinsley (1972) and Searle, Sargent, & Bagnuolo (1973), spectral population synthesis has become a standard technique to study the stellar populations of galaxies. Since stellar clusters can be assumed single age and single metallicity group of stars, their integrated colors reflect their age and metallicity for a given initial mass function. A comprehensive compilation of various evolutionary synthesis models was presented by Leitherer et al. (1996) and Kennicutt (1998). One of the widely used models is BC96. In this model, the evolution of the spectrophotometric properties for a wide range of stellar metallicity, $Z = 0.0004, 0.004, 0.008, 0.02, 0.05$, and 0.1, are presented. The evolving spectra include the contribution of the stellar component in the range from the EUV to the FIR. The age varies from 0 to 20 Gyr and various IMFs are considered.

To estimate the ages of star clusters in M33, we convolve the SED of BC96 with BATC filter profiles to obtain the optical and near-infrared integrated luminosity. The integrated luminosity $L_{\lambda_i}(t, Z)$ of the i th BATC filter can be calculated as

$$L_{\lambda_i}(t, Z) = \frac{\int F_\lambda(t, Z) \varphi_i(\lambda) d\lambda}{\int \varphi_i(\lambda) d\lambda}, \quad (4)$$

where $F_\lambda(t, Z)$ is the SED of the BC96 of metallicity Z at age t , $\varphi_i(\lambda)$ is the response functions of the i th filter of the BATC filter system ($i = 3, 4, \dots, 15$), respectively. To avoid using distance-dependent parameters, we calculate the integrated colors of a BC96 relative to the BATC filter BATC08 ($\lambda = 6075\text{\AA}$):

$$C_{\lambda_i}(t, Z) = L_{\lambda_i}(t, Z) / L_{6075}(t, Z). \quad (5)$$

As a result, we obtain intermediate-band colors for 6 metallicities from $Z = 0.0004$ to $Z = 0.1$. Then, we determined the ages and best-fit models of metallicity by minimizing the difference between the intrinsic and integrated colors of BC96,

$$R^2(n, t, Z) = \sum_{i=3}^{15} [C_{\lambda_i}^{\text{intr}}(n) - C_{\lambda_i}^{\text{ssp}}(t, Z)]^2, \quad (6)$$

where $C_{\lambda_i}^{\text{ssp}}(t, Z)$ represents the integrated color in the i th filter of a SSP with age t and metallicity Z , and $C_{\lambda_i}^{\text{intr}}(n)$ is the intrinsic integrated color for n th star cluster. For convenience, we also list the ages of sample star clusters of this paper in Column 5 of Table 4. The uncertainties in the age estimates arising from photometric uncertainties are 0.2 or so, i.e., $\text{age} \pm 0.2 \times \text{age}$ [log yr], and are formal errors that do not include the model uncertainties. The star cluster ages obtained in this paper are model-dependent and do not represent “absolute values”. Uncertainties exist in the stellar evolution, in the physics of the stellar structure and

in the spectral libraries. For example, Charlot, Worthey, & Bressan (1996) evaluated the uncertainties in stellar population synthesis models by analyzing in detail the origin of the discrepancies between three models (Bertelli et al. 1994; Worthey 1994; BC96), and showed the main uncertainties originate from the underlying stellar evolution theory, the color-temperature scale of giant stars, and the flux libraries. Cardiel et al. (2003) also discussed in detail the problem of disentangling stellar population properties using the spectroscopic data. Vazdekis et al. (2001) investigated the origin of the discrepancy between the spectroscopic age and the CMD age for the Milky Way GC 47 Tuc, and found that the α -enhanced isochrones with atomic diffusion included can provide a good fit to the CMD of 47 Tuc and lead to a spectroscopic age in better agreement with the CMD age.

4. Metallicity estimates

4.1. Correlation between color index and metallicity

To study the integrated properties of the stellar population in M81, Kong et al. (2000) used the simple stellar population synthesis models of BC96. First, they convolved the SEDs of BC96 with the BATC filter profiles to obtain the optical and near-infrared integrated luminosity. When they plot the relations between color and age, they found that, among all the BATC filter bands, the color index centered at 8510Å is much more sensitive to the metallicity than to the age (see Fig. 3 of Kong et al. 2000 for details). The center of this filter band (8510Å) is near the CaT. A good relationship between the flux ratio of $I_{8510} \equiv L_{8510}/L_{9170}$ and the metallicity for stellar populations older than 1 Gyr was found (Eq. (4) of Kong et al. 2000),

$$Z = (0.83 - 0.84 \times I_{8510})^2. \quad (7)$$

4.2. Results

Using equation (7), we can calculate the metallicities of these old star clusters. We obtained $I_{8510} \equiv L_{8510}/L_{9170}$ using the photometric magnitudes in BATC13 and BATC14 bands (see Table 3). Then, the metallicities can be obtained using equation (7). The results are listed in Table 4 ($[\text{Fe}/\text{H}] = \log Z - \log Z_{\odot}$). The uncertainties for the metallicities are just the formal errors, since Kong et al. (2000) did not discuss any errors and uncertainties when they derived Eq. (7). The formal errors are obtained in the following way. Random values are selected for the observed data such that they obey a normal distribution, with sigma determined by the known errors in each sampled bin. We then obtain the best-fit metallicity. This procedure was repeated 300 times, giving us 300 separate determinations of the best-fit metallicity. The statistical standard deviation of metallicity from this procedure is adopted as the final error for the metallicity. In Table 4, we also present the ages for the sample clusters from Ma

et al. (2001, 2002a,b,c). Table 5 lists some sample cluster metallicities from other authors (Cohen, Persson, & Searle 1984; Christian & Schommer 1988; Brodie & Huchra 1991; Sarajedini et al. 1998). Using two reddening-independent techniques, Cohen, Persson, & Searle (1984) obtained abundance estimates for the four GCs, M9, U49, H38, and C20. Comparing the results for these four clusters, we find that the only very discrepant result is for M9, which we derive to be moderately metal rich, while Cohen, Persson, & Searle (1984) estimated it to be very metal poor. However, the results of Christian & Schommer (1988) and Sarajedini et al. (1998) for M9 are intermediate between Cohen, Persson, & Searle (1984) and this study. Christian & Schommer (1988) and Brodie & Huchra (1991) estimated the metallicities for the 10 GCs using integrated spectra. The mean metallicity difference (the values of this paper minus the values of Christian & Schommer 1988 and Brodie & Huchra 1991) is $< \Delta[\text{Fe}/\text{H}] > = 0.153 \pm 0.192$. Sarajedini et al. (1998) estimated the metallicities for these 10 GCs based on the shape and color of the red giant branch. Our results are consistent with Sarajedini et al. (1998) except for C38, which we find is very metal poor, but Sarajedini et al. (1998) find it to be the most metal rich. The mean metallicity difference (the values of this paper minus the values of Sarajedini et al. 1998) is $< \Delta[\text{Fe}/\text{H}] > = 0.148 \pm 0.216$. Sarajedini et al. (2000) estimated the cluster metallicities using the integrated $B - V$ colors from Christian & Schommer (1988) and the equations of Couture, Harris, & Allwright (1990), and presented that the metallicity of R12 is very metal rich. Except for this cluster, our results are also consistent with the ones obtained using $B - V$ colors, and the mean difference ($< [\text{Fe}/\text{H}]_{\text{This paper}} - [\text{Fe}/\text{H}]_{B-V} >$) is 0.056 ± 0.273 .

5. Some properties of old star clusters

The following statistical relations are based on our data and are thus model-dependent.

5.1. Metallicity as a function of deprojected distance

Vilchez et al. (1988) studied the abundance gradient in M33 on the data of emission lines in selected HII regions. The O/H gradient is steep in the inner regions, but much flatter in the outer regions, and N/O is constant over most of the visible disk, but lower in the outer HII region. We can investigate the radial abundance behavior of the old clusters in M33. Using the data of both the red and blue portions of the instability strip of two halo globular clusters (M9 and U77) and the RR Lyrae luminosity relation, Sarajedini et al. (2000) estimated M33 to be at a distance of $(m - M)_0 = 24.84 \pm 0.16$, which is adopted in this paper. We also adopted the inclination and position angles to be 56° and 23° of M33, respectively (Regan & Vogel 1994). When the line of intersection (i.e. the major axis of

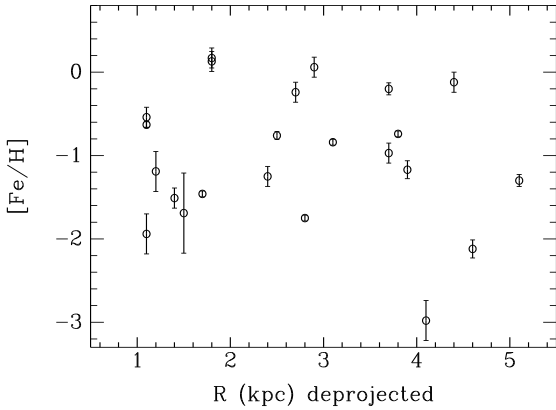


Fig. 2. Deprojected radial variation of metal abundance for 23 “true” GCs of M33.

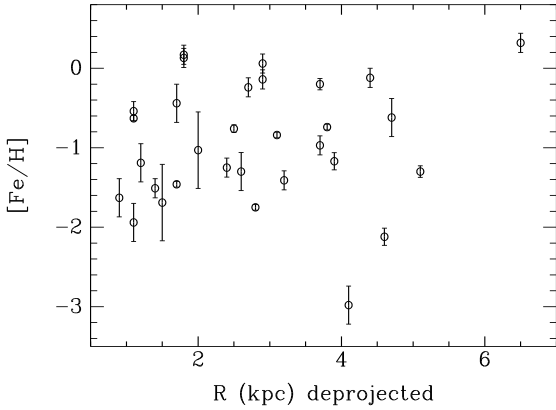


Fig. 3. Deprojected radial variation of metal abundance for 31 old clusters of M33.

the image) between the galactic plane and tangent plane is taken as the polar axis, it is easily proved that

$$r = \rho \sqrt{1 + \tan^2 \gamma \sin^2 \theta} \quad (8)$$

and

$$\tan \phi = \frac{\tan \theta}{\cos \gamma}, \quad (9)$$

where r and ϕ are the polar co-ordinates in the galactic plane, and ρ and θ are the corresponding co-ordinates in the tangent plane, and γ is the inclination angle of the galactic disk. Using formula (8), we can obtain the distances of our sample clusters from the center of M33. Figure 2 displays the variation of metal abundance with deprojected radial position in units of kpc for 23 globular cluster candidates in M33. This figure presents no relationship between the metal abundance of a cluster and its distance from the galactic center. This conclusion is consistent with that in Sarajedini et al. (2000) for the 9 GCs in this galaxy. Figure 3 plots the variation of metal abundance with deprojected radial position for all old clusters in this study.

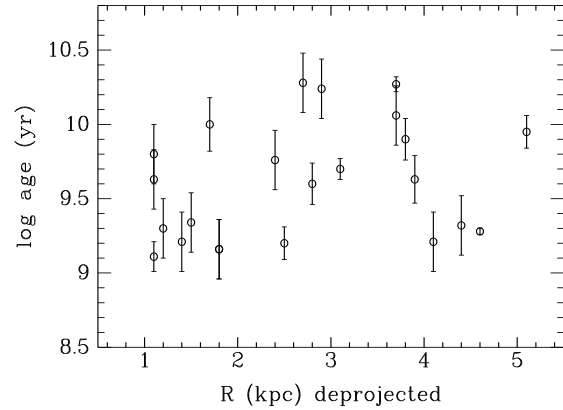


Fig. 4. Age as a function of galactocentric distance for 23 “true” GCs of M33.

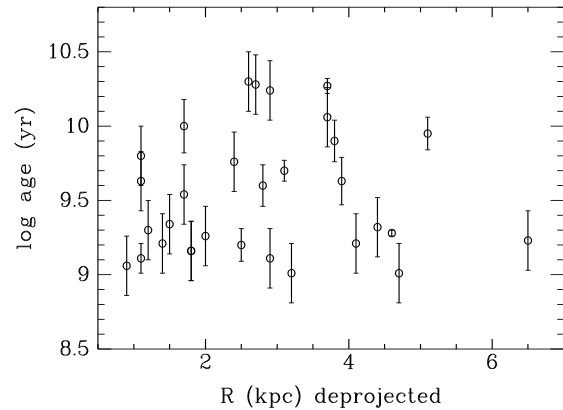


Fig. 5. Age as a function of galactocentric distance for 31 old clusters of M33.

5.2. Age as a function of deprojected distance

In Figure 4, we plot the relation between age and galactocentric distance for 23 “true” GCs of M33. Here we note that no relationship exists. This conclusion is consistent with Sarajedini & King (1989) and Chaboyer, Demarque, & Sarajedini (1996) for the GCs in the Galaxy. Figure 5 shows this relation for all 31 old clusters in this study, and no relationship can be found, too.

6. Summary and discussion

In this paper, based on the results of multicolor spectrophotometry in Ma et al. (2001, 2002a, 2001b, 2002c) and on the formula of Kong et al. (2000), we estimate the metallicities of 31 old star clusters in M33, of which there are 23 “true” GCs. The results show that most of these old clusters are metal poor. At the same time, we compare our results with others (Cohen, Persson, & Searle 1984; Christian & Schommer 1988; Brodie & Huchra 1991; Sarajedini et al. 1998) derived using different methods, such as integrated spectra and photometry. In general, our results are consistent. The statistical results show that, the

ages and metal abundances based on our data do not vary with deprojected radial position.

As we know, the old stellar populations and the nuclei of spiral galaxies are dominated by G, K and M stars and therefore emit bulk of their light in the near infrared region of the spectrum. The CaT feature has been the subject of several analyses. Different authors emphasized its different utilizations, such as a luminosity indicator, and a possible discriminator between the light contribution due to dwarfs and giants in a given population mix (Idiart et al. 1997). Bica & Alloin (1987) presented CCD spectra with 12.5Å resolution for 30 star clusters, and measured the near-infrared continuum distribution and the equivalent widths of 13 absorption features. They found that in the near-infrared spectral range, metallicity is the dominant parameter. Based on the analysis of stars (giant stars, supergiants and dwarfs), star clusters, and galaxy nuclei, Alloin & Bica (1989) showed that the equivalent widths of CaT are metallicity dependent, although not as much as other metallic or molecular features (CN or Mg+MgH). Armandroff & Zinn (1988) found that the strength of the CaT in the integrated spectra of GCs forms a one-parameter family, this parameter being the metallicity. Erdelyi-Mendes & Barbuy (1991) calculated synthetic spectra for the Ca II lines in the local thermodynamic equilibrium approximation using the model atmospheres computed by interpolation in the grids of models by Gustafsson et al. (1975) and an unpublished grid of dwarf models (see Erdelyi-Mendes & Barbuy 1991 for details). By a detailed analysis of the behavior of the strength of Ca II lines as a function of stellar parameters, Erdelyi-Mendes & Barbuy (1991) concluded that CaT has a weak dependence on the effective temperature, a modest dependence on surface gravity, but a quite important dependence on metallicity, i.e., an exponential dependence between the flux of the 2 strongest Ca II lines ($\lambda\lambda$ 8542Å and 8662Å) and metallicity. Mallik (1994) presented the observations of the infrared triplet lines of ionized Ca for 91 stars in the spectral range F8 – M4 of all luminosity classes and in the metallic range $-0.65 - +0.60$, and found that the dependence of the CaT fluxes on gravity and metallicity is intricately connected, but for supergiants a strong relationship can be found. He also indicated that when a large metallicity range is considered (i.e. ≥ 1.0 dex), the influence of the metallicity on the CaT becomes conspicuous. Idiart et al. (1997) also confirmed the strong dependence of CaT index on metallicity.

Acknowledgements. We would like to thank the anonymous referee for his/her insightful comments and suggestions that improved this paper. This work has been supported by the National Key Basic Research Science Foundation (NKBRSF TG199075402) and in part by the National Science Foundation

References

Alloin, D., & Bica, E. 1989, A&A, 217, 57
 Armandroff, T. E., & Zinn, R. 1988, AJ, 96, 92
 Bertelli, G., Bressan, A., Chiosi, C., Fagotto, F., & Nasi, E. 1994, A&AS, 106, 275
 Bica, E., & Alloin, D. 1987, A&A, 186, 49
 Brodie, J., & Huchra, J. 1991, ApJ, 379, 157
 Cardiel, N., et al. 2003, A&A, in print (astro-ph/0306560)
 Chandar, R., Bianchi, L., & Ford, H. C. 1999a, ApJS, 122, 431
 Chandar, R., Bianchi, L., & Ford, H. C. 1999b, ApJ, 517, 668
 Chandar, R., Bianchi, L., Ford, H. C., & Salasnich, B. 1999c, PASP, 111, 794
 Chandar, R., Bianchi, L., & Ford, H. C. 2001, A&A, 366, 498
 Chandar, R., Bianchi, L., Ford, H. C., & Sarajedini, A. A. 2002, ApJ, 564, 712
 Charlot, S., Worthey, G., & Bressan, A. 1996, ApJ, 457, 625
 Christian, C. A., & Schommer, R. A. 1982, ApJS, 49, 405
 Christian, C. A., & Schommer, R. A. 1988, AJ, 95, 704
 Cohen, J. G., Persson, S. E., & Searle, L. 1984, ApJ, 218, 141
 Couture, J., Harris, W. E., & Allwright, J. W. B. 1990, ApJS, 73, 671
 Erdelyi-Mendes, M., & Barbuy, B. 1991, A&A, 241, 176
 Fan, X. H., et al. 1996, AJ, 112, 628
 Fukugita, M., et al. 1996, AJ, 111, 1748
 Gustafsson, B., Bell, R. A., Eriksson, K., & Nordlund, A. 1975, A&A, 42, 407
 Hiltner, W. A. 1960, ApJ, 131, 163
 Idiart, T. P., Thévenin, F., & de Freitas Pacheco, J. A. 1997, AJ, 113, 1066
 Huchra, J., Brodie, J., Caldwell, N., Christian, C., & Schommer, R. 1996, ApJS, 102, 29
 Kaluzny, J., Stanek, K. Z., Krockenberger, M., Sasselov, D., Tonry, J. L., & Mateo, M. 1998, AJ, 115, 1016
 Kennicutt, R. C. 1998, ARA&A, 36, 189
 Kong, X., et al. 2000, AJ, 119, 2745
 Kron, G. E., & Mayall, N. U. 1960, AJ, 65, 581
 Leitherer, C., et al. 1996, PASP, 108, 996
 Ma, J., et al. 2001, AJ, 122, 1796
 Ma, J., Zhou, X., Chen, J., Wu, H., Jiang, Z., Xue, S., & Zhu, J. 2002a, A&A, 385, 404
 Ma, J., Zhou, X., Chen, J., Wu, H., Jiang, Z., Xue, S., & Zhu, J. 2002b, AJ, 123, 3141
 Ma, J., et al. 2002c, Acta Astron., 52, 453
 Mallik, S.V. 1994, A&AS, 103, 279
 Melnick, J., & D'Odorico, S. 1978, A&AS, 34, 249
 Mochejska, B. J., Kaluzny, J., Krockenberger, M., Sasselov, D. D., & Stanek, K. Z. 1998, Acta Astron., 48, 455
 Oke, J. B., & Gunn, J. E. 1983, ApJ, 266, 713
 Regan, M. W., & Vogel, S. N. 1994, ApJ, 434, 536
 Searle, L., Sargent, W. L. W., & Bagnuolo, W. G. 1973, ApJ, 179, 427
 Sarajedini, A. A., & King, C. R. 1989, AJ, 98, 1624
 Sarajedini, A. A., Geisler, D., Harding, P., & Schommer, R. 1998, ApJ, 508, L37
 Sarajedini, A. A., Geisler, D., Schommer, R., & Harding, P. 2000, AJ, 120, 2437
 Schommer, R. A., Christian, C. A., Caldwell, N., Bothun, G. D., & Huchra, J. 1991, AJ, 101, 873
 Stanek, K. Z., Kaluzny, J., Krockenberger, M., Sasselov, D. D., Tonry, J. L., & Mateo, M. 1998, AJ, 115, 1894
 Tinsley, B. M. 1972, A&A, 20, 382
 van den Bergh, S. 1991, PASP, 103, 609
 van den Bergh, S. 1999, ARA&A, 9, 273

Vazdekis, A., Salaris, M., Arimoto, N., & Rose, J. A. 2001,
ApJ, 549, 274

Vilchez, J. M., Pagel, B. E. J., Díaz, A. I., Terlevich, E., &
Edmunds, M. G. 1988, MNRAS, 235, 633

Worthey, G. 1994, ApJS, 95, 107

Yan, H. J., et al. 2002, PASP, 112, 691

Zheng, Z. Y., et al. 1999, AJ, 117, 2757

Zhou, X., Jiang, Z. J., Xue, S. J., Wu, H., Ma, J., & Chen, J.
S. 2001, ChJAA, 1, 372

Zhou, X. 1991, A&A, 248, 367

Table 1. Comparison age estimates with previous measurements

Cluster ^a	Chandar et al. log age (yr)	Ma et al. log age (yr)
U49	9.2 ± 0.1	9.60
R12	9.7 ± 0.1	10.00
R14	10.2 ± 0.2	9.11
M9	9.2 ± 0.1	9.63
U77	9.15 ± 0.15	9.20
H38	9.25 ± 0.15	9.70
C20	9.2 ± 0.1	9.95
C38	8.9 ± 0.1	9.28
H10	9.25 ± 0.15	9.90
U137	9.35 ± 0.15	10.27
CBF11	9.50 ± 0.30	10.30
CBF20	10.1 ± 0.20	9.54
CBF22	9.25 ± 0.15	9.26
CBF28	10.2 ± 0.40	9.80
CBF49	7.90 ± 0.20	9.34
CBF59	7.40 ± 0.20	9.11
CBF69	9.2 ± 0.1	9.76
CBF74	9.3 ± 0.1	9.32
CBF97	9.3 ± 0.2	10.28
CBF112	8.8 ± 0.2	9.21
CBF118	9.15 ± 0.15	9.16
CBF161	9.1 ± 0.1	9.23
M12	9.4 ± 0.2	9.63

^a CBF identifications are from Chandar, Bianchi, & Ford (1999a, 2001); M identifications are from Mochejska et al. (1998); The others are from Christian & Schommer (1982).

Table 2. Parameters of the BATC Filters and Statistics of Observations

No.	Name	cw ^a (Å)	Exp. (hr)	N.img ^b	rms ^c
1	BATC03	4210	00:55	04	0.024
2	BATC04	4546	01:05	04	0.023
3	BATC05	4872	03:55	19	0.017
4	BATC06	5250	03:19	15	0.006
5	BATC07	5785	04:38	17	0.011
6	BATC08	6075	01:26	08	0.016
7	BATC09	6710	01:09	08	0.006
8	BATC10	7010	01:41	08	0.005
9	BATC11	7530	02:07	10	0.017
10	BATC12	8000	03:00	11	0.003
11	BATC13	8510	03:15	11	0.005
12	BATC14	9170	04:45	25	0.011
13	BATC15	9720	05:00	26	0.009

^a Central wavelength for each BATC filter

^b Image numbers for each BATC filter

^c Zero point error, in magnitude, for each filter as obtained from the standard stars

Table 3. SEDs of 31 Old Star Clusters

Cluster ^a (1)	03 (2)	04 (3)	05 (4)	06 (5)	07 (6)	08 (7)	09 (8)	10 (9)	11 (10)	12 (11)	13 (12)	14 (13)	15 (14)
U49	16.99 0.022	16.56 0.018	16.46 0.014	16.27 0.015	16.06 0.010	15.98 0.011	15.82 0.011	15.78 0.010	15.70 0.010	15.58 0.009	15.52 0.010	15.48 0.012	15.40 0.012
R12	17.34 0.049	16.81 0.036	16.62 0.027	16.43 0.029	16.15 0.020	16.11 0.021	15.90 0.022	15.83 0.023	15.77 0.022	15.68 0.019	15.56 0.021	15.51 0.020	15.44 0.024
R14	17.55 0.052	17.04 0.037	16.84 0.027	16.59 0.028	16.21 0.019	16.14 0.021	15.91 0.017	15.81 0.018	15.66 0.020	15.55 0.016	15.43 0.017	15.32 0.017	15.20 0.021
M9	17.82 0.046	17.48 0.034	17.38 0.025	17.17 0.026	16.96 0.016	16.90 0.018	16.73 0.016	16.68 0.018	16.60 0.018	16.53 0.017	16.45 0.025	16.39 0.021	16.38 0.026
U77	17.94 0.066	17.51 0.047	17.38 0.042	17.20 0.039	17.05 0.025	16.97 0.024	16.77 0.033	16.75 0.024	16.68 0.030	16.59 0.028	16.58 0.030	16.49 0.031	16.41 0.044
H38	18.03 0.035	17.68 0.028	17.52 0.021	17.27 0.020	17.06 0.016	16.99 0.016	16.80 0.015	16.71 0.015	16.69 0.016	16.61 0.015	16.55 0.022	16.46 0.019	16.49 0.026
C20	18.44 0.037	18.05 0.026	17.87 0.022	17.70 0.022	17.50 0.017	17.42 0.020	17.24 0.017	17.26 0.020	17.13 0.019	17.00 0.019	16.90 0.025	16.84 0.021	16.81 0.039
C38	18.71 0.080	18.35 0.050	18.28 0.040	18.05 0.058	17.98 0.029	17.88 0.040	17.78 0.032	17.70 0.037	17.73 0.034	17.73 0.041	17.80 0.058	17.80 0.061	17.72 0.089
H10	19.27 0.093	18.73 0.055	18.54 0.043	18.21 0.038	17.96 0.030	17.76 0.030	17.53 0.033	17.51 0.031	17.31 0.029	17.21 0.029	17.19 0.033	17.10 0.036	17.03 0.053
U137	19.21 0.082	18.88 0.058	18.68 0.043	18.42 0.043	18.22 0.030	18.10 0.030	17.88 0.029	17.80 0.031	17.81 0.033	17.74 0.036	17.71 0.049	17.54 0.042	17.61 0.065
CBF11	19.56 0.153	19.05 0.098	18.99 0.080	18.82 0.085	18.50 0.063	18.52 0.075	18.19 0.052	18.11 0.053	17.99 0.050	17.95 0.067	17.67 0.081	17.62 0.046	17.54 0.071
CBF20	19.11 0.102	18.76 0.077	18.70 0.063	18.45 0.063	18.31 0.054	18.25 0.061	18.05 0.048	17.83 0.043	17.70 0.040	17.71 0.055	17.52 0.072	17.39 0.038	17.30 0.058
CBF22	18.66 0.065	18.23 0.046	18.13 0.037	18.01 0.040	17.76 0.032	17.79 0.038	17.74 0.035	17.63 0.034	17.60 0.035	17.49 0.043	17.56 0.071	17.49 0.040	17.32 0.056
CBF28	17.26 0.024	16.75 0.017	16.60 0.013	16.46 0.014	16.16 0.010	16.15 0.012	15.97 0.010	15.91 0.010	15.87 0.010	15.78 0.011	15.72 0.015	15.69 0.010	15.66 0.014
CBF49	19.37 0.151	18.54 0.073	18.56 0.065	18.52 0.078	18.08 0.049	18.07 0.057	17.86 0.046	17.91 0.050	17.93 0.054	17.74 0.059	17.80 0.094	17.81 0.059	17.75 0.090
CBF59	18.47 0.046	18.29 0.038	18.28 0.034	18.19 0.037	17.92 0.033	17.98 0.036	17.87 0.031	17.69 0.029	17.48 0.026	17.38 0.034	17.34 0.050	17.16 0.028	17.05 0.041
CBF69	19.36 0.154	19.10 0.125	18.99 0.135	18.53 0.155	18.62 0.100	18.48 0.088	18.34 0.093	18.28 0.087	18.19 0.099	18.21 0.103	17.96 0.106	17.90 0.102	18.08 0.163
CBF74	19.93 0.201	19.43 0.142	19.14 0.095	18.87 0.100	18.68 0.064	18.59 0.069	18.47 0.064	18.40 0.068	18.41 0.072	18.16 0.061	18.28 0.098	18.09 0.076	18.08 0.101
CBF77	18.53 0.061	18.33 0.045	18.35 0.039	18.04 0.046	18.08 0.032	17.80 0.036	17.82 0.030	17.82 0.036	17.64 0.035	17.50 0.028	17.57 0.049	17.46 0.037	17.09 0.054
CBF87	19.91 0.143	19.44 0.090	19.22 0.060	18.96 0.057	18.89 0.045	18.68 0.051	18.53 0.051	18.45 0.052	18.50 0.055	18.35 0.047	18.19 0.072	18.23 0.075	18.28 0.102

Table 3. Continued

Cluste ^a (1)	03 (2)	04 (3)	05 (4)	06 (5)	07 (6)	08 (7)	09 (8)	10 (9)	11 (10)	12 (11)	13 (12)	14 (13)	15 (14)
CBF87	19.91 0.143	19.44 0.090	19.22 0.060	18.96 0.057	18.89 0.045	18.68 0.051	18.53 0.051	18.45 0.052	18.50 0.055	18.35 0.047	18.19 0.072	18.23 0.075	18.28 0.102
CBF97	19.18 0.125	18.81 0.105	18.64 0.091	18.49 0.086	18.29 0.067	18.17 0.068	17.83 0.063	17.79 0.059	17.72 0.069	17.61 0.057	17.53 0.065	17.37 0.056	17.44 0.094
CBF112	19.08 0.082	18.79 0.071	18.74 0.059	18.51 0.063	18.49 0.053	18.40 0.056	18.33 0.059	18.33 0.065	18.22 0.071	18.04 0.063	18.08 0.080	18.07 0.082	18.17 0.161
CBF118	18.32 0.163	18.00 0.154	17.88 0.123	17.66 0.126	17.52 0.091	17.39 0.094	17.27 0.087	17.13 0.084	17.05 0.084	17.10 0.084	16.97 0.089	16.72 0.066	16.78 0.089
CBF119	18.48 0.160	18.16 0.154	18.09 0.122	17.87 0.126	17.72 0.093	17.60 0.094	17.54 0.096	17.34 0.082	17.26 0.086	17.31 0.081	17.16 0.086	16.90 0.063	16.95 0.089
CBF130	17.67 0.089	17.32 0.078	17.48 0.079	17.22 0.089	17.43 0.087	17.06 0.080	16.85 0.066	16.81 0.075	16.78 0.086	17.13 0.114	16.66 0.087	16.68 0.093	16.60 0.108
CBF131	18.27 0.113	17.87 0.089	17.87 0.074	17.75 0.079	17.54 0.052	17.48 0.054	17.32 0.049	17.32 0.052	17.32 0.061	17.34 0.058	17.21 0.069	17.24 0.077	17.08 0.085
CBF161	19.364 0.077	19.028 0.054	18.869 0.039	18.660 0.034	18.457 0.033	18.339 0.033	18.180 0.034	18.074 0.036	17.956 0.035	17.942 0.038	17.951 0.059	17.631 0.043	17.631 0.078
M5	19.17 0.084	18.70 0.051	18.52 0.037	18.28 0.043	18.05 0.031	17.94 0.034	17.78 0.032	17.63 0.036	17.63 0.037	17.53 0.035	17.61 0.050	17.38 0.038	17.42 0.076
M12	17.99 0.116	17.67 0.114	17.53 0.089	17.29 0.086	17.15 0.064	17.04 0.064	16.83 0.038	16.78 0.051	16.74 0.055	16.64 0.051	16.53 0.056	16.41 0.058	16.36 0.061
M33	17.06 0.045	16.65 0.034	16.52 0.026	16.35 0.031	16.16 0.022	16.11 0.024	15.97 0.022	15.93 0.022	15.87 0.023	15.74 0.020	15.69 0.022	15.64 0.021	15.53 0.024
M51	18.07 0.030	17.70 0.022	17.64 0.018	17.52 0.021	17.35 0.017	17.32 0.019	17.21 0.019	17.18 0.022	17.12 0.023	17.06 0.024	17.01 0.038	16.98 0.035	16.85 0.042

^a CBF identifications are from Chandar, Bianchi, & Ford (1999a, 2001); M identifications are from Mochejska et al. (1998); The others are from Christian & Schommer (1982).

Table 4. Metallicities of 31 old star clusters in M33

Cluster	$B - V$	$V - I$	[Fe/H]	log age (yr)
U49	0.68	1.029	-1.75 ± 0.036	9.60
R12	1.03	1.154	-1.46 ± 0.036	10.00
R14	0.98	1.311	-0.63 ± 0.036	9.11
M9	0.69	1.016	-1.17 ± 0.108	9.63
U77	0.67	0.994	-0.76 ± 0.048	9.20
H38	0.73	1.070	-0.84 ± 0.036	9.70
C20	0.77	1.045	-1.30 ± 0.072	9.95
C38	0.73	0.883	-2.12 ± 0.108	9.28
H10	0.96	1.243	-0.74 ± 0.036	9.90
U137	0.83	1.099	-0.20 ± 0.072	10.27
CBF11	-1.30 ± 0.240	10.30
CBF20	-0.44 ± 0.240	9.54
CBF22	0.513	...	-1.03 ± 0.481	9.26
CBF28	0.794	...	-1.94 ± 0.240	9.80
CBF49	0.824	...	-1.69 ± 0.481	9.34
CBF59	-0.14 ± 0.120	9.11
CBF69	...	1.061	-1.25 ± 0.120	9.76
CBF74	...	1.061	-0.12 ± 0.120	9.32
CBF77	...	0.438	-0.62 ± 0.240	9.01
CBF87	...	1.151	-0.97 ± 0.120	10.06
CBF97	...	1.015	-0.24 ± 0.120	10.28
CBF112	...	0.846	-2.98 ± 0.240	9.21
CBF118	...	0.983	0.13 ± 0.120	9.16
CBF119	...	0.940	0.17 ± 0.120	9.16
CBF130	...	0.667	-1.63 ± 0.240	9.06
CBF131	...	0.898	-1.19 ± 0.240	9.30
CBF161	0.32 ± 0.120	10.28
M5	0.73	1.32	0.06 ± 0.120	10.24
M12	0.66	1.11	-0.54 ± 0.120	9.63
M33	0.71	1.00	-1.51 ± 0.120	9.21
M51	0.64	0.65	-1.41 ± 0.120	9.01

Table 5. Comparison metallicity estimates with previous measurements

Cluster	[Fe/H] ^a	[Fe/H] _{CPS} ^b	[Fe/H] _{CS} ^c	[Fe/H] _{BH} ^d	[Fe/H] _S ^e
U49	-1.75 ± 0.036	-1.4	-0.8 ± 0.3	-1.70 ± 0.53	-1.64 ± 0.20
R12	-1.46 ± 0.036	...	-1.2 ± 0.3	...	-1.19 ± 0.24
R14	-0.63 ± 0.036	...	-1.5 ± 0.3	...	-1.00 ± 0.50
M9	-1.17 ± 0.108	-2.2	-1.7 ± 0.3	...	-1.64 ± 0.28
U77	-0.76 ± 0.048	-1.77 ± 0.77	-1.56 ± 0.30
H38	-0.84 ± 0.036	-1.0	-1.5 ± 0.3	...	-1.10 ± 0.10
C20	-1.30 ± 0.072	-1.1	-2.2 ± 0.3	-1.25 ± 0.79	-1.25 ± 0.22
C38	-2.12 ± 0.108	...	-1.2 ± 0.3	...	-0.65 ± 0.16
H10	-0.74 ± 0.036	-0.91 ± 0.90	-1.44 ± 0.26
U137	-0.20 ± 0.072	-0.12 ± 0.38	-0.98 ± 0.16

^a This paper

^b Cohen, Persson, & Searle 1984

^c Christian & Schommer 1988

^d Brodie & Huchra 1991

^e Sarajedini et al. 1998

This figure "majunfig1.jpg" is available in "jpg" format from:

<http://arxiv.org/ps/astro-ph/0503615v1>

